Lithuanian Journal of Physics
Vol. **66**, No. 1, pp. 8–19 (2026)
ISSN 1648-8504 eISSN 2424-3647
DOI: https://doi.org/10.3952/physics.2026.66.1.2

THERMOPHILIC PROTEINS – EXPLORING THERMAL STABILITY OF FN3 DOMAIN FROM *THERMOANAEROBACTER TENGCONGENSIS* BASED ON *IN SILICO* EXPERIMENTS

C. Barman, A. Jezierska, and J.J. Panek

Faculty of Chemistry, University of Wrocław, ul. F. Joliot-Curie 14, 50-383 Wrocław, Poland
Email: jaroslaw.panek@uwr.edu.pl

Received 31 October 2025; accepted 25 November 2025

Extremophilic proteins exhibit a remarkable stability under extreme conditions (e.g. thermophilic systems are stable at elevated temperatures), offering insights into molecular adaptations and early life on Earth. Currently, thermophilic organisms are widely investigated, and they constitute a challenge for new industrial and pharmaceutical applications. Examples of studies on extremophiles, including thermophiles, reach as far as space exploration experiments. The Fibronectin Type 3 (FN3) domain, a conserved structural motif, plays key roles in protein interactions and stability. This study investigates the thermal stability of the FN3 domain from the thermophilic bacterium *Thermoanaerobacter tengcongensis.* The domains of the wild type and its triple mutant FN3 were simulated (Protein Data Bank ids: 7JGT and 7JGU, respectively), with a wild-type human analogue (Protein Data Bank id: 5KF4) as a control, using molecular dynamics (MD) with classical force field. The simulations were performed at 300, 350 and 400 K temperatures to show their impact on the molecular properties. Structural parameters were analyzed, including root mean square deviation (RMSD), root mean square fluctuations (RMSF), solvent accessible surface area (SASA), secondary structure assignment and hydrogen bond networks. The obtained results reveal that the thermophilic bacterial variants of the FN3 domain exhibit lower structural fluctuations, particularly in residues 10–20 and 50–60, compared to the human analogue. The bacterial FN3 mutant exhibited reduced stability compared to the wild type, highlighting the importance of hydrogen bonding network in ensuring thermal stability. These findings enhance our understanding of the molecular mechanisms underlying the stability and adaptation of extremophilic proteins to high temperatures.

Keywords: thermophilic proteins, mesophilic proteins, extremophiles, FN3 domain, secondary structure, salt bridges, molecular dynamics, classical force fields, RMSD, RMSF, SASA

PACS: 36.20.Ey, 31.15.xv

1. Introduction

Extremophilic proteins are a remarkable class of biomolecules derived from extremophiles – organisms that thrive in environments once considered inhospitable to life. These environments include extremes of temperature, pH, pressure, salinity and radiation [1]. The study of extremophilic proteins has garnered a significant scientific interest due to their extraordinary stability and functionality under conditions that would typically denature or inactivate proteins from mesophilic organisms [2]. Understanding the structural and functional adaptations of these proteins not only provides insights into the limits of life but also opens doors to innovative biotechnological and industrial applications [3, 4]. Current enzymatic processes are mostly based on the enzymes isolated from mesophilic organisms, which might not exhibit optimal activity at the conditions of the industrial process. There are several examples of successful industrial applications of extremophiles. Extremophilic DNA polymerases from *Thermococcus litoralis*, *Thermus aquaticus* and *Pyrococcus furiosus* have already found a widespread use in the polymerase chain reaction (PCR), a crucial tool in DNA analysis, useful not only in biotechnology, but also in medicine and criminology [5]. Bioleaching – extraction of metals (mostly copper

and gold) from sulfide ores – is also already important, accounting for ca. 10% of copper mining; the harsh conditions of the process (temperature and acidity) call for the use of extremophilic organisms [6]. Production of three carotenoids, β-carotene, bacteriorhodopsin and canthaxanthin, can be efficiently achieved with microbes thriving in high-salinity solutions [7]. Finally, diverse organisms of the genera *Caldicellulosiruptor*, *Pyrococcus*, *Thermoanaerobacterium* and *Aeropyrum* are tested for the synthesis of biofuels, e.g. conversion of plant sugars (xylose and hemicellulose) to ethanol [8].

Extremophilic proteins are categorized based on the extreme conditions where their host organisms inhabit:

- Thermophilic proteins: derived from organisms that thrive in high-temperature environments (45–122°C), such as hot springs and hydrothermal vents.
- Psychrophilic proteins: found in organisms living in extremely cold environments, such as polar regions and deep oceans.
- Acidophilic and alkaliphilic proteins: originating from organisms that survive in highly acidic (pH < 3) or alkaline (pH > 9) conditions, respectively.
- Halophilic proteins: derived from organisms that inhabit high-salinity environments, such as salt lakes and saline soils.
- Piezophilic (barophilic) proteins: found in organisms that thrive under high-pressure conditions, such as deep-sea environments.
- Radioresistant proteins: derived from organisms that withstand high levels of ionizing radiation [9].

The stability and functionality of extremophilic proteins are attributed to specific structural adaptations. For example, thermophilic proteins often feature increased hydrophobic interactions, extensive hydrogen bonding networks, and a higher prevalence of ionic interactions, which confer thermal stability [10]. In contrast, psychrophilic proteins exhibit increased flexibility, allowing them to function at low temperatures, while halophilic proteins possess a high surface density of acidic residues to maintain solubility and function in high-salt environments [11]. These adaptations highlight the diverse strategies employed by extremophilic proteins to maintain stability and activity under extreme conditions [12]. The study of the mechanisms encounter many difficulties using *in silico* approaches, such as the limited time scale of the molecular dynamics simulations (currently reaching the microsecond regime) or difficulty in adjusting pH or ionic strength (salinity) within classical force fields. Nowadays, computational approaches are indispensable to study the structure and molecular properties of thermophilic proteins. However, they are limited to the homology modelling, e.g. protein structure prediction from the sequence of amino acids, when the three-dimensional experimental structures are unknown, classical molecular dynamics (MD) methods or application of machine learning (ML) to predict the structure and prepare the classification of the proteins [13–15]. Despite the mentioned problems, we applied the molecular dynamics method with force fields to estimate the stability and reveal molecular properties such as the network of hydrogen bonds influencing the thermophilic features in the fibronectin type III (FN3) domain.

The FN3 domain is a ubiquitous and evolutionarily conserved protein module found in a wide variety of proteins across diverse organisms, from bacteria to humans [16, 17]. First identified as a repeating structural unit in the extracellular matrix protein fibronectin, the FN3 domain has since been recognized as a key structural and functional component in many proteins involved in cell adhesion, signalling and mechanotransduction [18, 19]. Its modular architecture, stability and versatility make it a critical player in mediating protein–protein interactions and cellular processes.

The FN3 domain is characterized by a β-sandwich fold composed of seven β-strands arranged in two antiparallel β sheets, forming a compact and stable structure. This fold is highly adaptable, allowing the FN3 domain to participate in a wide range of biological functions [20]. Unlike other immunoglobulin-like domains, the FN3 domain lacks disulfide bonds, and this contributes to its stability and flexibility in diverse environments, including the extracellular matrix and intracellular compartments [18, 20].

The FN3 domain has been extensively studied in mesophilic organisms. However, recent discoveries have revealed the presence of FN3 domains in extremophiles – organisms that thrive in extreme

environments such as high temperatures, acidic or alkaline pH, high salinity and high pressure. These extremophilic FN3 domains exhibit unique structural and functional adaptations that enable them to maintain stability and functionality under conditions that would typically destabilize proteins from mesophilic organisms. The study of extremophilic FN3 domains not only expands our understanding of protein evolution and adaptation but also opens new avenues for biotechnological applications [21].

The unique properties of extremophilic FN3 domains make them attractive candidates for biotechnology. Their stability under extreme conditions can be harnessed for applications such as enzyme engineering, biosensing, and the development of synthetic binding proteins [22]. For example, thermostable FN3 domains could be used to design robust scaffolds for therapeutic proteins or industrial enzymes that operate at high temperatures. Similarly, halophilic FN3 domains may be exploited for applications in high-salt environments, such as bioremediation or food processing. The study of extremophilic FN3 domains also contributes to the growing field of protein engineering, where insights from natural adaptations are used to design proteins with novel functions [17, 18].

This paper aims to provide an overview of extremophilic FN3 domains, focusing on their structural changes in high temperatures. By examining these unique protein modules, we hope to highlight their significance in both basic science and biotechnology, as well as inspire further research into the mechanisms of protein stability and adaptation in extreme environments. We explore the thermal stability of FN3 or fibronectin type 3 protein domain from *Thermoanaerobacter tengcongensis* as wild type (PDB id: 7JGT) and the triple mutant in R23, R25 and R72 position (PDB id: 7JGU) [23] using molecular dynamics simulations. For control, we have taken into account a non-thermophilic system which is the human analogue of the FN3 domain (PDB id: 5KF4) [24] with a very similar fold (see Fig. 1). The most important structural descriptors such as root mean square deviation (RMSD), root mean square fluctuation (RMSF), solvent-accessible surface area (SASA) and H-bond network will be discussed taking into account the time evolution of these parameters, revealing differences between the systems studied.

2. Methods

2.1. Model preparation

The initial coordinates for the thermophilic FN3 domain wild type from *Thermoanaerobacter tengcongensis* and its triple mutant (R23, R25, R72) were obtained from the Protein Data Bank [25] (PDB ids: 7JGT and 7JGU, respectively [23]). The human FN3 domain (PDB id: 5KF4) was selected as a mesophilic control [24]. Each protein structure was solvated in a cubic box with explicit SPC/E water molecules [26]. The SPC/E model was shown to provide the best agreement with an experimental structure of water and hydration thermochemistry at elevated temperatures [27] in comparison with other models, including a faster, but more approximate TIP3P approach [28]. The systems were neutralized with Na^+ or Cl^- counterions, and an additional 0.15 M NaCl was added to mimic physiological ionic strength. The steps required for system preparation were

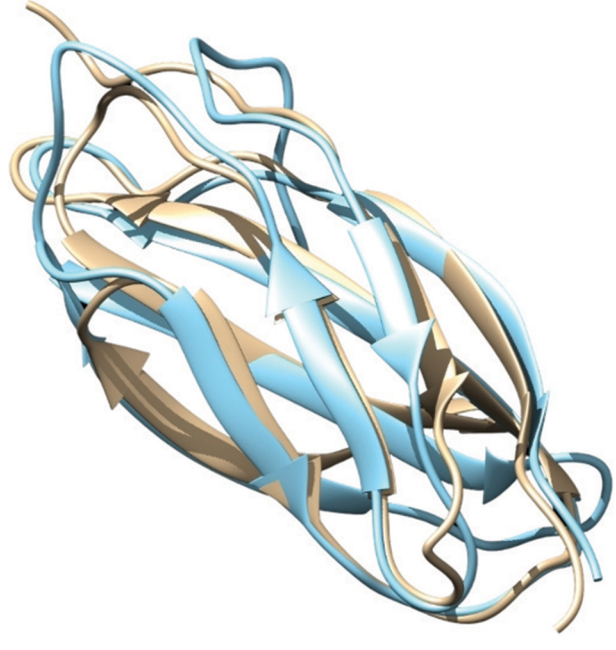

Fig. 1. Structural alignment of thermophilic (7JGT; tan-coloured ribbon) and human (5KF4; cyan ribbon) FN3 domains. The MatchMaker algorithm of UCSF Chimera 1.17.3 was used to align the sequences and then align the corresponding alpha carbon atoms of the structures.

carried out with the CHARMM-GUI web interface [29, 30].

The comparative assessment of thermal stability was carried out by the use of three independent systems for each protein variant. These systems were configured for MD simulations at three distinct temperatures: 300, 350 and 400 K. This temperature range was chosen to examine behaviour under physiological conditions (300 K) and under extreme conditions (400 K) that challenge the structural integrity of the proteins.

2.2. Molecular dynamics simulations

All simulations were performed using the GROMACS software package, Version 2024.2 [31]. The AMBER94 force field [32] was employed for the protein and ions, while the SPC/E model [26] was used for water molecules. Energy minimization was carried out using the steepest descent algorithm with a Verlet cutoff scheme, proceeding until the maximum force fell below 1000 kJ/mol/nm.

Following the minimization, the systems underwent a two-phase equilibration protocol. First, a 100 ps simulation in the NVT ensemble (constant number of particles, volume and temperature) was performed at 300 K, regulated by the V-rescale thermostat. This was followed by a 100 ps simulation in the NPT ensemble (constant number of particles, pressure and temperature) at 1 bar, maintained using the Parrinello–Rahman barostat.

Subsequent production MD simulations were run for 1000 ns per system at each of three temperatures (300, 350 and 400 K), which results in total nine systems. Long-range electrostatic interactions were handled using the Particle Mesh Ewald (PME) method. Bond lengths were constrained with the LINCS algorithm, permitting a 2 fs integration time step. The non-bonding interactions cutoff was set to 1 nm. Trajectory coordinates were saved every 10 ps for subsequent analysis. The post-processing was carried out including RMSD, RMSF and SASA analyses. In addition, the evolution of intermolecular H-bonds network evolution was estimated. The data analyses and graphical representation of the results were prepared with the use of GROMACS 2024.2 integrated tools [31], UCSF Chimera 1.17.3 [33] and VMD 1.9.3 [34] programs, as well as the Matlab R2025b mathematical package [35].

3. Results and discussion

In the current study, the molecular features of the FN3 domain are investigated from thermophilic protein and its mesophilic analogue. The proteins of the FN3 domain in this study are of bacterial (7JGT) and human (5KF4) origin. Nevertheless, the FN3 domain, which is a β-sandwich fold composed of seven β-strands arranged in two antiparallel β-sheets, is highly conserved structurally as seen in Fig. 1, where the two mentioned experimental structures are superimposed with an overall RMSD of 1.82 Å (calculated over 82 matching residues with the MatchMaker algorithm of the UCSF Chimera software).

The structural analysis based on the RMSD performed for the MD results obtained at 300 K for the human analogue (Fig. 2) ranges from ca. 0.12 to 0.21 nm confirming that the structure was preserved during the simulations. Taking into account the RMSD fluctuations, it is visible that the smallest deviations are noticed for the human analogue. All the cases studied are stable at the discussed temperature; however, the largest changes are noticed for the wild type (from ca. 0.07 to 0.27 nm). At the temperature raised by 50 K, we observe that the smallest changes in the RMSD value exhibits again the human analogue. However, we could notice that for ca. 300 ns of the simulations the values range between 0.12–0.24 nm. During the remaining time, the RMSD increased and oscillates between 0.24–0.38 nm. Significantly larger fluctuations were observed in the FN3 domain for the thermophilic proteins. In both cases (wild type and the triple mutant), we noticed an increase of the RMSD value during the simulation time. In the thermophilic wild type FN3 domain, the RMSD value range did not change for more than 400 ns of the simulation. Next, there is an increase registered between ca. 420 and 570 ns. Again, the RMSD values decreased, and after ca. 690 ns, a rapid increase was noticed. However, the RMSD values stabilized and ranged between 0.4–0.81 nm until the end of the simulation. For the triple mutant, the RMSD value was increasing for ca. 750 ns suggesting that the structure is getting unstable in the simulation time. However, during the last ca. 250 ns of the simulation, the value stopped to change significantly and fluctuated between 0.56 and

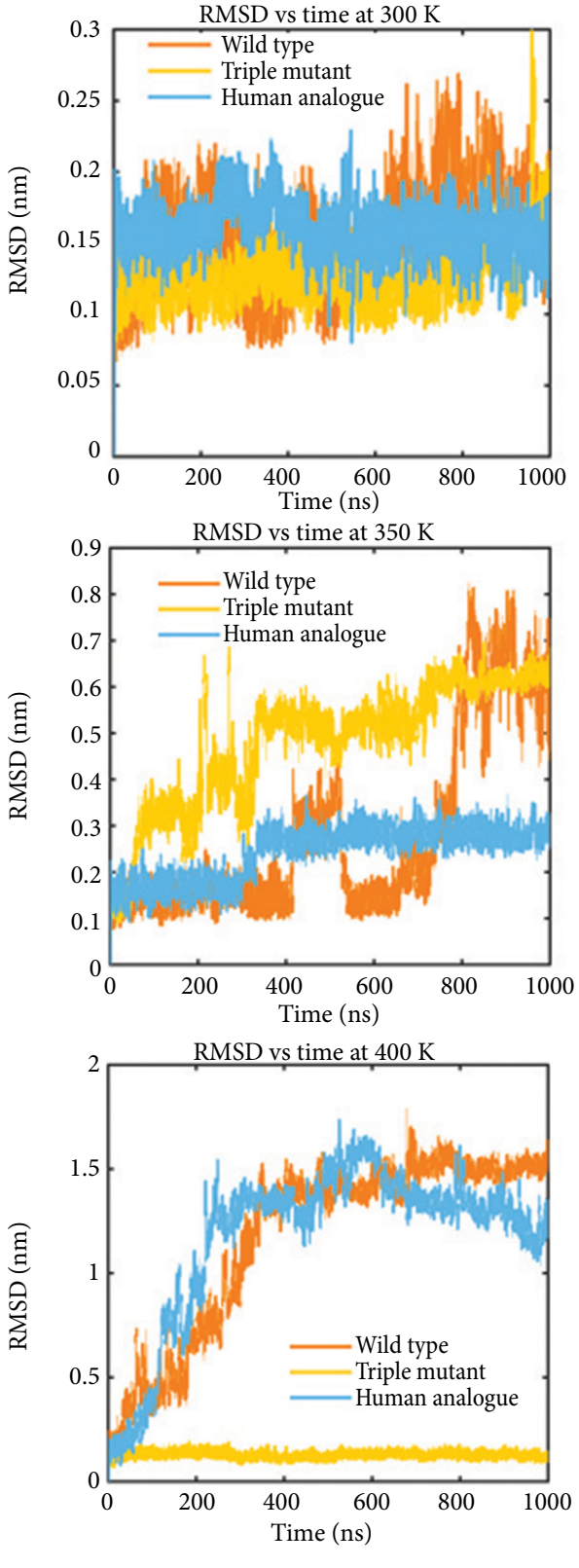

Fig. 2. Root mean square deviation (RMSD) at 300, 350 and 400 K obtained for the wild type and its triple mutant of the FN3 domain of thermophilic bacterium *Thermoanaerobacter tengcongensis* as well as for the wild-type human analogue (which served as a reference structure). The MD simulations were performed for 1000 ns.

0.7 nm. At the last temperature that we took into account in the investigations (400 K), the RMSD values of the triple mutant were stable during the whole simulation time. In the case of wild types of the studied systems, other observations were made. In both bacterial and human cases, a rapid increase of the RMSD was registered, as shown in Fig. 2, suggesting the instability of the analyzed proteins. The situation has changed after ca. 200 ns in the case of the human analogue, and after ca. 300 ns concerning the thermophilic wild type and we could notice smaller changes. Even, in the case of the human analogue, the RMSD values have started to decrease. Concluding this part of the analysis, we can say that in all investigated temperatures the analyzed proteins remained stable. This, however, is a result of the global indicator (RMSD) and will be verified using local structural descriptors.

RMSF was calculated for the studied cases at three temperatures used during the MD study (see Fig. 3). Let us start the discussion from the lowest temperature – 300 K. At this temperature for the human analogue, we could detect four regions with the strongest residue mobility compared to the thermophilic wild type and its triple mutant. They were detected close to 22–28, 45–57, 62–75 and 80–88 residues. Concerning the wild type of the thermophilic protein, we noticed four regions as well with the strongest mobility compared to the human analogue and the triple mutant. They were found for the residues initiating and ending the structure of the protein as well as close to 13–22 and 41–46 residues. From Fig. 3 one can see that the triple mutant residues exhibit the weakest mobility. We could see single amino acids showing larger fluctuations than their equivalents in other studied structures. In principle, we can distinguish two regions around amino acids 8–12 and 75–89. Concerning the 350 K temperature, one could notice that overall the highest RMSF is exhibited by the thermophilic wild type. However, we could observe three regions (close to residues 10–18, 38–44 and 62–68) with the highest RMSF values as well as in the terminal part of the protein. Elevated mobility of the terminal regions is not unexpected, and should not be dangerous to the integrity of the protein structure. Analyzing the human analogue, significant changes in the values of the parameter were found close to

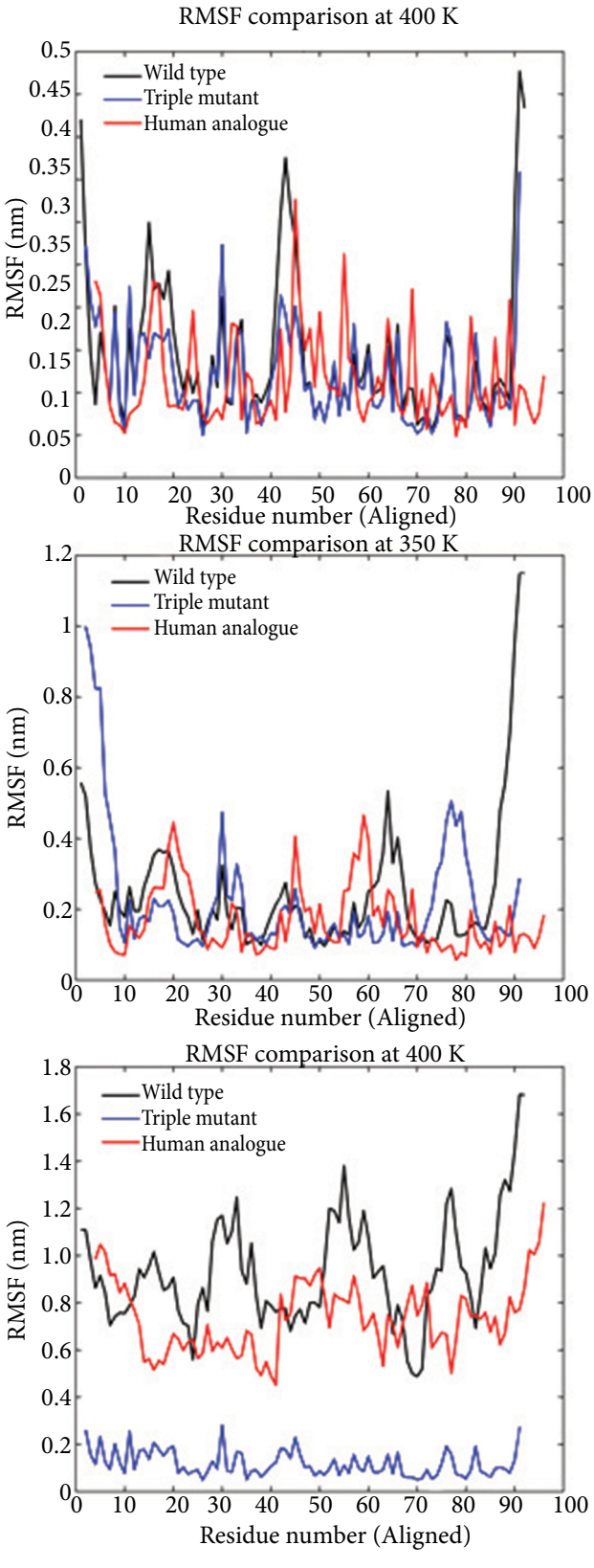

Fig. 3. Root mean square fluctuation (RMSF) at 300, 350 and 400 K obtained for the wild type and its triple mutant of the FN3 domain of thermophilic bacterium *Thermoanaerobacter tengcongensis* as well as for the wild-type human analogue (which served as a reference structure).

18–25, 44–52, 55–62 and 68–69 residues. In the triple mutant, strong fluctuations were detected for the initial part of the protein – the first ten amino acids. In addition, we could indicate two regions close to 28–35 and 72–83. The results for 300 and 350 K suggest in general that the β-strands form the stable core of the protein and are responsible for the regions of the lowest RMSF. In the last panel of Fig. 3, the data obtained for RMSF at 400 K are presented. The lowest fluctuations were found for the triple mutant of the thermophilic protein suggesting that it is most stable at the highest temperature. Concerning the wild types derived from mesophilic and thermophilic species, one can notice that at higher temperatures the fluctuations are very strong in both cases – even stronger for the thermophilic wild type. Even the β-sandwich fold core seems to undergo large fluctuations, which could mean its unfolding.

In the next step, SASA was analyzed. The SASA is discussed based on the data collected at three temperatures as previously. The obtained results after 1000 ns of the simulation time are presented in Fig. 4. At room temperature, lower SASA values were noticed for the human analogue compared to thermophilic species. The detected area ranges from ca. 53 to 61 nm^2. It is interesting that the SASA analysis gave almost equivalent results for the thermophilic proteins indicating that the triple mutation had not affected the real structure. It is impossible to distinguish between the wild type and the triple mutant from the obtained data (see Fig. 4). However, the solvent-accessible area ranges from ca. 54 to 64.5 nm^2 being higher compared to the human analogue. This suggests that the structures of the proteins are less stable and more flexible. Additionally, this means that they are more exposed to the solvent. An increase of the temperature to 350 K revealed that the solvent-accessible area for the human analogue has changed to a small extent. It ranges mostly between 52.5 and 62 nm^2. This suggests that even at higher temperature the structure is preserved. Higher values of SASA are noticed for both thermophilic systems indicating that the structures are more exposed to the solvent (less stable more unfolded). Generally, during the simulation time, in the wild type of the thermophilic protein, the solvent-accessible area fluctuated from 53 to 67 nm^2. For the triple mutant, the values

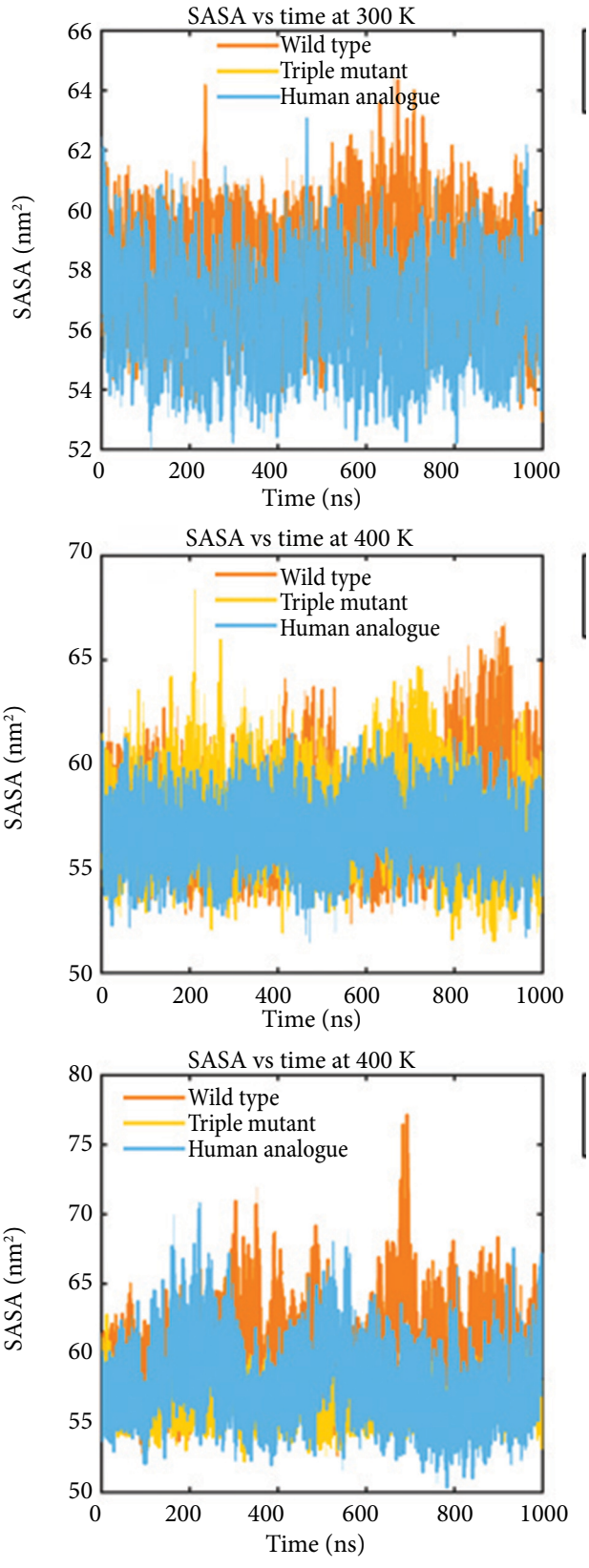

Fig. 4. Solvent-accessible surface area (SASA) at 300, 350 and 400 K obtained for the wild type and its triple mutant of the FN3 domain of thermophilic bacterium *Thermoanaerobacter tengcongensis* as well as for the wild-type human analogue (which served as a reference structure).

oscillated between 52.5 and 64 nm^2. Further increase of the temperature (see the last panel of Fig. 4) caused the destabilization of the human analogue structure. The SASA values became higher and during the simulation time they fluctuated from the value close to 50 nm^2 to almost 68 nm^2 (or for a moment exceeding 70 nm^2). The highest changes were detected for the wild type of the thermophilic protein confirming the structural changes related to the increase of the temperature. It is interesting to notice that the triple mutant exhibits very similar values of the SASA compared to the reference structure – human analogue.

Non-covalent interactions are of a great importance in nature. They play a significant role in the structural stabilization of biologically relevant systems. Therefore, we were interested to see how the network of the intermolecular hydrogen bonds evaluates during the simulation time. In Fig. 5, the changes of hydrogen bonds (HBs) number as a function of time are presented. The data were analyzed taking into account three different temperatures as in previous analyses. Based on classical force field, we could only analyze the changes of the distances between atoms involved in the formation of intermolecular hydrogen bond. At room temperature, the variation of formed hydrogen bonds is smallest in the human analogue, while the number of HBs itself is largest. It ranges between 35 and 47 during the simulation time. Concerning the thermophilic proteins, they exhibit a richer diversification of the network of the H-bonding – from 27 to 44 – while the running average number is consistently smaller than in the human analogue. Analyzing the figure, one can see that the number of hydrogen bonds does not differ much between the two thermophilic species. At the 350 K temperature, again we observe that the lower variation of hydrogen bonds concerns the human analogue. In the case of the thermophilic proteins, the variability of the hydrogen bonds is larger, moreover, it is worth noting that it is similar in the two discussed cases. At the highest temperature (the last panel of Fig. 5), the increase of the hydrogen bonds formation is noticed in the wild types of human analogue and the thermophilic protein, respectively. The number of the H-bonds in the triple mutant is not changing significantly during the simulation time. It is remarkable that the number of HBs is

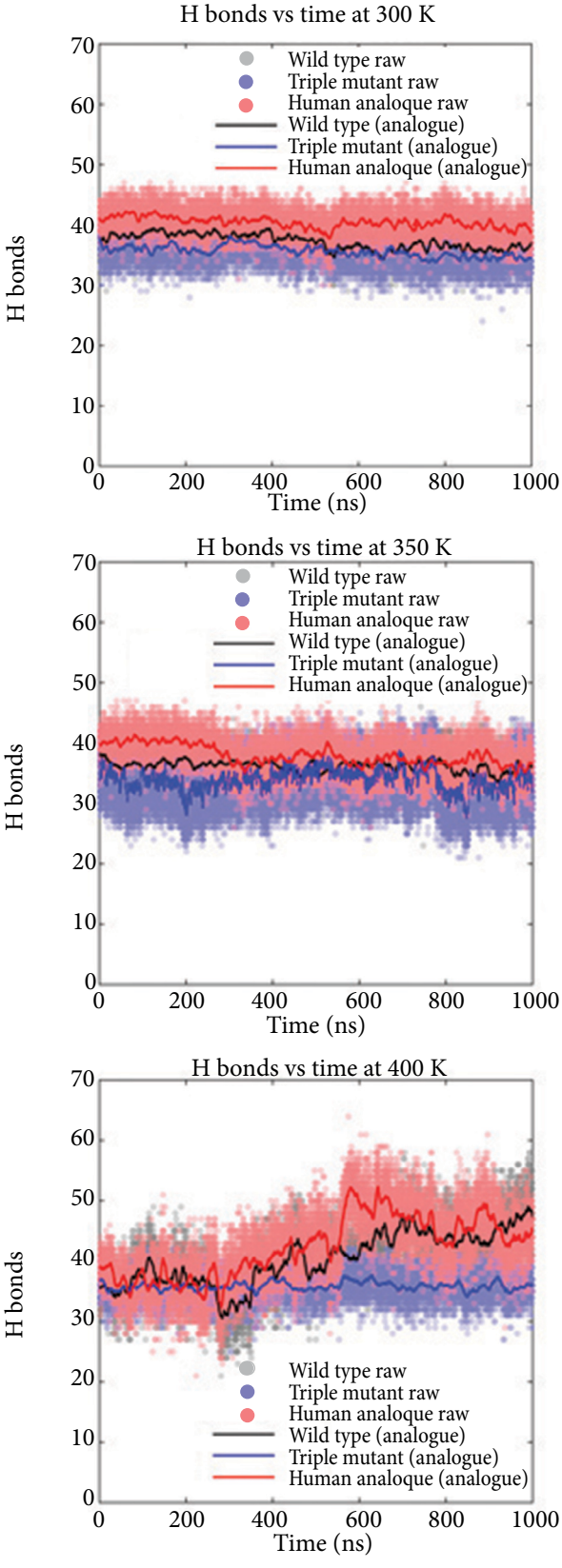

Fig. 5. Hydrogen bonds time evolution at 300, 350 and 400 K obtained for the wild type and its triple mutant of the FN3 domain of thermophilic bacterium *Thermoanaerobacter tengcongensis* as well as for the wild-type human analogue (which served as a reference structure).

increasing in the case of 400 K simulations, where the secondary structure of the wild-type proteins is changing (see below). This is the case where structural reorganization due to the kinetic energy brought by the elevated temperature is reflected not in breaking the HB network, but rather by its complete change. The *in silico* experiments consider the kinetic energy of the system as the parameter by which the macroscopic temperature is controlled and measured, so the thermostatting of the system is performed via algorithms of velocity rescaling.

The structural indicators described so far are related to the global (RMSD, SASA) and local (RMSF) integrity of the protein, but the most important factor to be considered is the secondary structure. The STRIDE algorithm [36], implemented in the VMD program [34] used within the current study, involves the empirical, geometrical hydrogen bond energy formula as well as the backbone torsional angle terms. The results of the secondary structure assignments along the MD trajectory for each simulation are presented in Fig. 6. The results for the 300 K runs (the top row of Fig. 6) show that all the proteins (two thermophilic variants: the wild type and its triple mutant, and the human analogue) are stable and the β-strands connected by short turn regions are preserved. The situation is slightly different at 350 K (the middle row of Fig. 6). At this temperature, the thermophilic wild-type protein is most stable structurally. Some distortions are recorded for the triple mutant, where three turn regions undergo helicalization. This phenomenon is even more evident for the human analogue, where the distortions expand already at ca. 250 ns of the MD run to the β-strands. The final round of simulations (the bottom row of Fig. 6, 400 K) results in a fast disintegration of the β-sandwich core, progressing from the terminal and turn regions. The FN3 domain does not contain disulfide bonds, therefore the result corresponds to the reorganization of hydrogen bonds and loss of salt bridges. These facts are true for the wild type proteins, while the triple mutant surprisingly remained stable – its structural elements remained intact even at 400 K. The results of the secondary structure analysis are important in supplementing the picture provided by the global and local numerical indicators, since e.g. the RMSD graphs indicate large deviations from the initial structure, while the secondary elements remain, however, conserved.

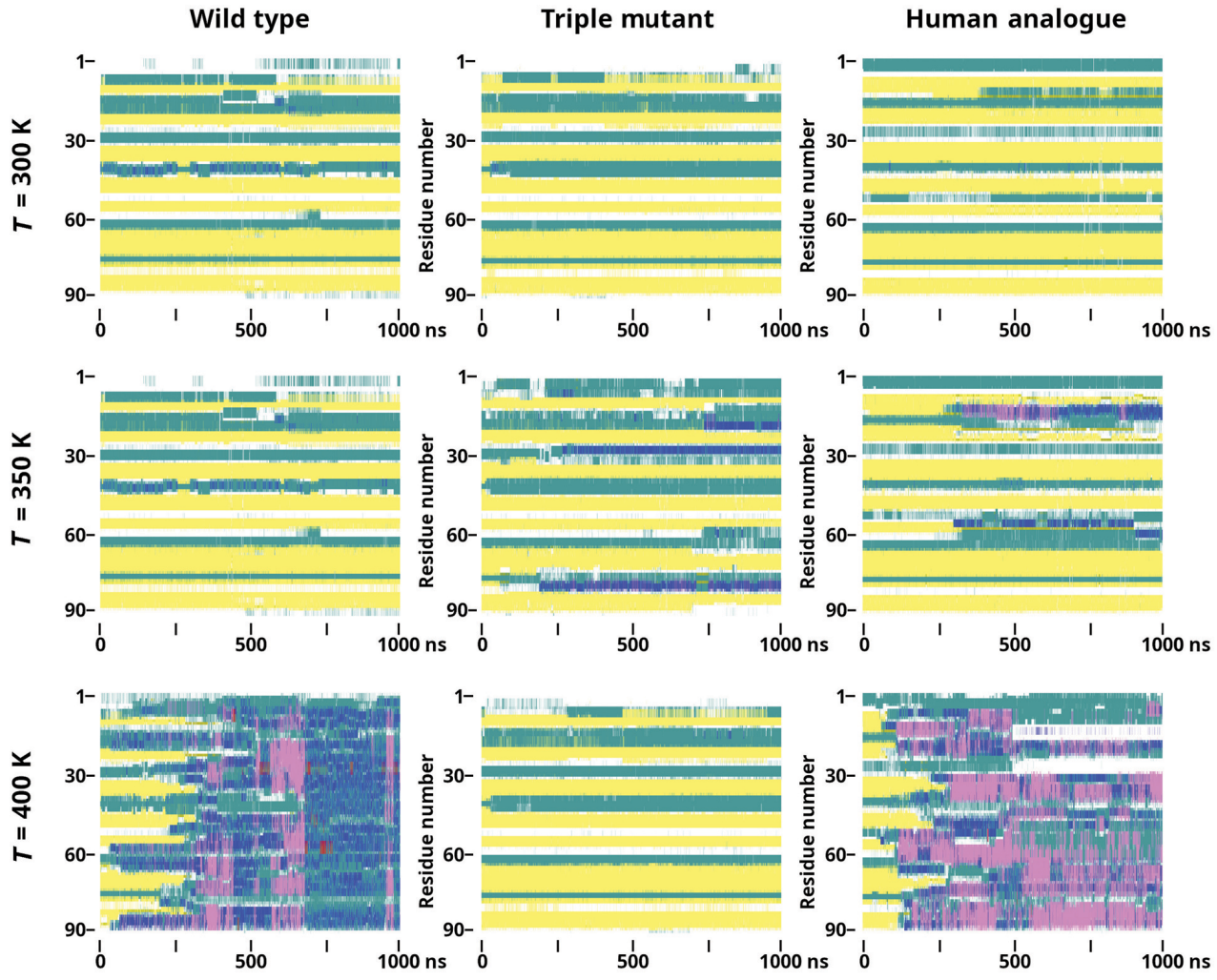

Fig. 6. Secondary structure changes at 300, 350 and 400 K obtained for the wild type and its triple mutant of the FN3 domain of thermophilic bacterium *Thermoanaerobacter tengcongensis* as well as for the wild-type human analogue (which served as a reference structure). Vertical axis: residue number; horizontal axis: simulation time in ns. Colour coding of the secondary structures: yellow, β-sheet; magenta, α-helix; turquoise, turn; blue, 3_{10} helix; red, π-helix; white, random coil.

4. Conclusions

The RMSF for the three systems suggests that the human analogue exhibits much stronger mobility especially close to the residues 10–20 and 50–60. The FN3 mutant is also less stable than the wild type protein stressing the importance of the hydrogen bonding interactions for thermal stability. The RMSD global parameter indicates that the proteins at elevated temperatures undergo structural changes. Their nature is revealed by the secondary structure analysis – at 350 K, the thermophilic wild type is most stable, while the human analogue shows the largest structural deviations. At 400 K, however, the bacterial and human wild types are quickly unfolded and within ca. 300 ns the secondary structure corresponding to the FN3 domain is not existent anymore. This result shows the potential of computer simulations to study the stability of proteins in extreme conditions.

Acknowledgements

We gratefully acknowledge the Polish high-performance computing infrastructure PLGrid Academic Computer Centre Cyfronet AGH) for providing computer facilities and support within Computational Grant No. PLG/2024/017802.

References

[1] G. Marzban and D. Tesei, The extremophiles: Adaptation mechanisms and biotechnological applications, Biology **14**, 412 (2025), https://doi.org/10.3390/biology14040412

[2] T. Satyanarayana, J. Littlechild, and Y. Kawarabayasi (eds.), *Thermophilic Microbes in Environmental and Industrial Biotechnology: Biotechnology of Thermophiles*, 2nd ed. (Springer Science+Business Media, Dordrecht, 2013).

[3] M. de Champdoré, M. Staiano, M. Rossi, and Sabato D'Auria, Proteins from extremophiles as stable tools for advanced biotechnological applications of high social interest, J. R. Soc. Interface **14**, 183–191 (2006), https://doi.org/10.1098/rsif.2006.0174

[4] A. Kumar, A. Alam, D. Tripathi, M. Rani, H. Khatoon, S. Pandey, N.Z. Ehtesham, and S.E. Hasnain, Protein adaptations in extremophiles: An insight into extremophilic connection of mycobacterial proteome, Sem. Cell Devel. Biol. **175**, 103660 (2025), https://doi.org/10.1016/j.semcdb.2025.103660

[5] H. Zhu, H. Zhang, Y. Xu, S. Laššáková, M. Korabečná, and P. Neužil, PCR past, present and future, Biotechniques **69**, 317–325 (2020), https://doi.org/10.2144/btn-2020-0057

[6] L.H. Gracioso, J. Peña-Bahamonde, B. Karolski, B.B. Borrego, E.A. Perpetuo, C.A.O. do Nascimento, H. Hashiguchi, M.A. Juliano, F.C. Robles Hernandez, and D.F. Rodrigues, Copper mining bacteria: Converting toxic copper ions into a stable single-atom copper, Sci. Adv. **7**, eabd9210 (2021), https://doi.org/10.1126/sciadv.abd9210

[7] M. Rodrigo-Baños, I. Garbayo, C. Vílchez, M.J. Bonete, and R.M. Martínez-Espinosa, Carotenoids from Haloarchaea and their potential in biotechnology, Mar. Drugs **13**, 5508–5532 (2015), https://doi.org/10.3390/md13095508

[8] F. Sepe, E. Costanzo, E. Ionata, and L. Marcolongo, Biotechnological potential of extremophiles: Environmental solutions, challenges, and advancements, Biology **14**, 847 (2025), https://doi.org/10.3390/biology14070847

[9] J.A. Coker, 'All About' extremophiles, Fac. Rev. **12**, 27 (2023), https://doi.org/10.12703/r/12-27

[10] R. Das and M. Gerstein, The stability of thermophilic proteins: A study based on comprehensive genome comparison, Funct. Integr. Genomics **1**, 76–88 (2000), https://doi.org/10.1007/s101420000003

[11] A. Saini, A. Kumar, G. Singh, and S.K. Giri, Survival strategies and stress adaptations in halophilic archaebacteria, in: *Microbial Stress Response: Mechanisms and Data Science*, eds. S.S. Dhiman, E.Z. Gnimpieba, and V. Gadhamshetty (American Chemical Society, Washington, DC, 2023) pp. 1–21.

[12] A. Maiti, S. Erimban, and S. Daschakraborty, Extreme makeover: The incredible cell membrane adaptations of extremophiles to harsh environments, Chem. Commun. **60**, 10280–10294 (2014), https://doi.org/10.1039/D4CC03114H

[13] Z. Chen, H. Wang, R. Wang, and Y. Qi, ThermoSeek: An integrated web resource for sequence and structural analysis of proteins from thermophilic species, J. Chem. Inf. Model. **65**, 5827–5838 (2025), https://doi.org/10.1021/acs.jcim.5c00010

[14] T. Zeiske, K.A. Stafford, and A.G. Palmer, III, Thermostability of enzymes from molecular dynamics simulations, J. Chem. Theory Comput. **12**(6), 2489–2492 (2016), https://doi.org/10.1021/acs.jctc.6b00120

[15] C. Feng, Z. Ma, D. Yang, X. Li, J. Zhang, and Y. Li, A method for prediction of thermophilic protein based on reduced amino acids and mixed features, Front. Bioeng. Biotechnol. **8**, 285 (2020), https://doi.org/10.3389/fbioe.2020.00285

[16] P. Bork and R.F. Doolittle, Proposed acquisition of an animal protein domain by bacteria, Proc. Natl. Acad. Sci. USA **89**, 8990–8994 (1992), https://doi.org/10.1073/pnas.89.19.8990

[17] A. Koide, C.W. Bailey, X. Huang, and S. Koide, The fibronectin type III domain as a scaffold for novel binding proteins, J. Mol. Biol. **284**, 1141–1151 (1998), https://doi.org/10.1006/jmbi.1998.2238

[18] L. Bloom, and V. Calabro, FN3: A new protein scaffold reaches the clinic, Drug Disc. Today

14, 949–955 (2009), https://doi.org/10.1016/j.drudis.2009.06.007

[19] S. Bencharit, C. Bin Cui, A. Siddiqui, E.L. Howard-Williams, J. Sondek, K. Zuobi-Hasona, and I. Aukhil, Structural insights into fibronectin type III domain mediated signaling, J. Mol. Biol. **367**, 303–309 (2013), https://doi.org/10.1016/j.jmb.2006.10.017

[20] R. Shah, T. Ohashi, H.P. Erickson, and T.G. Oas, Spontaneous unfolding-refolding of fibronectin type III domains assayed by thiol exchange, J. Biol. Chem. **292**, 955–966 (2017), https://doi.org/10.1074/jbc.M116.760371

[21] L.E. Petrovskaya, A.V. Zlobinov, L.N. Shingarova, E.F. Boldyreva, S.Sh. Gapizov, K.A. Novototskaya-Vlasova, E.M. Rivkina, D.A. Dolgikh, and M.P. Kirpichnikov, Fusion with the cold-active esterase facilitates autotransporter-based surface display of the 10th human fibronectin domain in *Escherichia coli*, Extremophiles **22**, 141–150 (2018), https://doi.org/10.1007/s00792-017-0990-7

[22] G. Gallo, R. Puopolo, M. Carbonaro, E. Maresca, and G. Fiorentino, Extremophiles, a nifty tool to face environmental pollution: From exploitation of metabolism to genome engineering, Int. J. Environ. Res. Public Health **18**, 5228 (2021), https://doi.org/10.3390/ijerph18105228

[23] L. Boucher, S. Somani, C. Negron, W. Ma, S. Jacobs, W. Chan, T. Malia, G. Obmolova, A. Teplyakov, G.L. Gilliland, and J. Luo, Surface salt bridges contribute to the extreme thermal stability of an FN3-like domain from a thermophilic bacterium, Proteins **90**, 270–281 (2022), https://doi.org/10.1002/prot.26218

[24] J. Zhao, J. Ren, N. Wang, Z. Cheng, R. Yang, G. Lin, Y. Guo, D. Cai, Y. Xie, and X. Zhao, Crystal structure of the second fibronectin type III (FN3) domain from human collagen α1 type XX, Acta Cryst. **F73**, 695–700 (2017), https://doi.org/10.1107/S2053230X1701648X

[25] H.M. Berman, J. Westbrook, Z. Feng, G. Gilliland, T.N. Bhat, H. Weisig, I.N. Shindyalov, and P.E. Bourne, The Protein Data Bank, Nucl. Acids Res. **28**, 235–242 (2000), https://doi.org/10.1093/nar/28.1.235

[26] H.J.C. Berendsen, J.R. Grigera, and T.P. Straatsma, The missing term in effective pair potentials, J. Phys. Chem. **91**, 6269–6271 (1987), https://doi.org/10.1021/j100308a038

[27] D. Paschek, Temperature dependence of the hydrophobic hydration and interaction of simple solutes: An examination of five popular water models, J. Chem. Phys. **120**, 6674–6690 (2004), https://doi.org/10.1063/1.1652015

[28] W.L. Jorgensen, J. Chandrasekhar, J.D. Madura, R.W. Impey, and M.L. Klein, Comparison of simple potential functions for simulating liquid water, J. Chem. Phys. **79**, 926–935 (1983), https://doi.org/10.1063/1.445869

[29] S. Jo, T. Kim, V.G. Iyer, and W. Im, CHARMM-GUI: A web-based graphical user interface for CHARMM, J. Comput. Chem. **29**, 1859–1865 (2008), https://doi.org/10.1002/jcc.20945

[30] J. Lee, M. Hitzenberger, M. Rieger, N.R. Kern, M. Zacharias, and W. Im, CHARMM-GUI supports the Amber force fields, J. Chem. Phys. **153**, 035103 (2020), https://doi.org/10.1063/5.0012280

[31] H.J.C. Berendsen, D. van der Spoel, and R. van Drunen, GROMACS: A message-passing parallel molecular dynamics implementation, Comp. Phys. Comm. **91**, 43–56 (1995), https://doi.org/10.1016/0010-4655(95)00042-E

[32] W.D. Cornell, P. Cieplak, C.I. Bayly, I.R. Gould, K.M. Merz Jr., D.M. Ferguson, D.C. Spellmeyer, T. Fox, J.W. Caldwell, and P.A. Kollman, A second generation force field for the simulation of proteins, nucleic acids, and organic molecules, J. Am. Chem. Soc. **117**, 5179–5197 (1995), https://doi.org/10.1021/ja00124a002

[33] E.F. Pettersen, T.D. Goddard, C.C. Huang, G.S. Couch, D.M. Greenblatt, E.C. Meng, and T.E. Ferrin, UCSF Chimera – a visualization system for exploratory research and analysis, J. Comput. Chem. **25**, 1605–1612 (2004), https://doi.org/10.1002/jcc.20084

[34] W. Humphrey, A. Dalke, and K. Schulten, VMD – visual molecular dynamics, J. Molec. Graphics **14**, 33–38 (1996), https://doi.org/10.1016/0263-7855(96)00018-5

[35] *MATLAB (R2023a) Computer Software* (The MathWorks, Inc., 2025), https://www.mathworks.com

[36] D. Frishman and P. Argos, Knowledge-based protein secondary structure assignment, Proteins **23**, 566–579 (1995), https://doi.org/10.1002/prot.340230412

TERMOFILINIAI BALTYMAI – *THERMOANAEROBACTER TENGCONGENSIS* FN3 DOMENO TERMINIO STABILUMO TYRIMAS REMIANTIS *IN SILICO* METODAIS

C. Barman, A. Jezierska, J.J. Panek

Vroclavo universiteto Chemijos fakultetas, Vroclavas, Lenkija